SpaceOps-2025, ID # 53

Trajectory Design for a Mission to Venus Using a Resonant Orbit to Land on a Desired Site on the Planet's Surface

Vladislav A. Zubko[a,*], Natan A. Eismont[b], Konstantin S. Fedyaev[c], Ravil R. Nazirov[d], Lydmila V. Zasova[e], Dmitriy A. Gorinov[f], Andrey A. Belyaev[g], Vladimir N. Nazarov[h]

[a] *Space Research Institute of the Russian Academy of Sciences, 84/32 Profsoyuznaya Str., Moscow, 117997, Russian Federation, v.zubko@cosmos.ru*
[b] *Space Research Institute of the Russian Academy of Sciences, 84/32 Profsoyuznaya Str., Moscow, 117997, Russian Federation, neismont@cosmos.ru*
[c] *Space Research Institute of the Russian Academy of Sciences, 84/32 Profsoyuznaya Str., Moscow, 117997, Russian Federation, kfedyaev@cosmos.ru*
[d] *Space Research Institute of the Russian Academy of Sciences, 84/32 Profsoyuznaya Str., Moscow, 117997, Russian Federation, rnazirov@cosmos.ru*
[e] *Space Research Institute of the Russian Academy of Sciences, 84/32 Profsoyuznaya Str., Moscow, 117997, Russian Federation, zasova@cosmos.ru*
[f] *Space Research Institute of the Russian Academy of Sciences, 84/32 Profsoyuznaya Str., Moscow, 117997, Russian Federation, gorinov@cosmos.ru*
[g] *Space Research Institute of the Russian Academy of Sciences, 84/32 Profsoyuznaya Str., Moscow, 117997, Russian Federation, a.belyaev@cosmos.ru*
[h] *Space Research Institute of the Russian Academy of Sciences, 84/32 Profsoyuznaya Str., Moscow, 117997, Russian Federation, vnazarovcosmos.ru*
* Corresponding Author

Abstract

One of the challenges associated with exploring the planet is a selection of the most suitable location for landing on the surface to collect highly accurate scientific data. However, due to both purely ballistic constraints such as the entry angle of the lander and launch opportunities as well as natural restrictions such as slow rotation of the planet, this choice reduces locations attainable for landing only to a few sites.

This paper presents a thorough investigation of flight trajectories to Venus, which were constructed via the methods of employing the gravity assist of the planet and the combination of resonant heliocentric orbital manifolds to guide the spacecraft towards the designated landing site. The study involves analysing the requirements for a working satellite in a near-Venus orbit, starting from technical specifications and progressing toward their mathematical interpretation. These resulting dependencies serve as the basis for the subsequent computation of potential landing sites on the planetary surface.

A comparative analysis of attainable landing sites obtained through classical approaches (direct flight) and those achieved via a technique involving gravity assist was conducted. This analysis revealed that the flight scheme proposed in this study offers advantages over traditional approaches, even when selecting landing sites is limited by the constraints of the orbiter's nominal orbit.

.

Keywords: Gravity assists, Venus exploration, resonant orbits, attainable landing sites, Venus orbiter, orbit dynamics

Nomenclature

$\{a, e, i, \omega, \Omega, f\}$ = the classical set of Keplerian elements for the satellite orbit around Venus is: semimajor axis, eccentricity, inclination, argument of periapsis, longitude of ascending node (or right ascension of the ascending node), and true anomaly. These elements are referenced to a frame in which the *x*-axis lies along the line connecting centers of masses of Venus and the Sun, and the *z*-axis is in the direction of the orbital momentum of Venus. Therefore, the plane of the Sun's motion coincides with the *xy* plane.

$\{a_0, e_0, i_0, \omega_0, \Omega_{,0} f_0\}$ = the initial values of Keplerian elements of the satellite orbit around Venus.

b = semi-minor axis of incoming hyperbolic orbit of the spacecraft, km.

C_3 = orbital energy of the spacecraft at Venus SOI boundary, km^2/s^2.

h_p = periapsis altitude of the satellite orbit around the Venus, km.

m, n = numbers determining the resonance ratio of heliocentric orbits of the satellite and Venus, i.e. such numbers that for n complete revolutions of Venus around the Sun the satellite makes exactly m revolutions at the heliocentric orbit.

$\mathbf{k}$ = vector pointing to the ascending node of the satellite orbit.

$\mathbf{r}$ = radius-vector of the spacecraft relative to Venus.

$\mathbf{r}_p$ = radius vector of a planet in the heliocentric ecliptic reference frame.

$r = \| \mathbf{r} \|$ = distance between centers of Venus and the spacecraft, km.

r_{SOI} = radius of the planets sphere of influence (SOI), km;

$r_\odot = \| \mathbf{r}_\odot \|$ = distance between centres of masses of Venus and the Sun, km.

$r_{10} = \| \mathbf{r} - \mathbf{r}_\odot \|$ satellite position relative to the Sun, km.

r_π = periapsis distance of the spacecraft trajectory relative to the planet.

T_1 = period of mutual visibility of an orbiter and a lander, s.

T_2 = ballistic lifetime of the orbiter, s.

$T_3 = T_3(\Omega_0, \omega_0)$ = duration of eclipse, s.

$\mathbf{v}$ = vector of the heliocentric velocity of the spacecraft when it approaches Venus in the heliocentric ecliptic reference frame; "+/-" upperscript denotes incoming and outgoing directions, respectively.

$\mathbf{v}_p$ = vector of the planet's orbital velocity in the heliocentric ecliptic reference frame.

$\mathbf{v}_\infty$ = vector of the asymptotic velocity of the spacecraft at Venus in the planetocentric ecliptic reference frame.

v_∞ = magnitude of the vector $\mathbf{v}_\infty$.

$\mathbf{v}_\infty^-$, $\mathbf{V}_\infty^+$ = vectors of incoming and outgoing asymptotic velocities of the spacecraft at Venus in the planetocentric ecliptic reference frame.

V_h = entry velocity into the Venusian atmosphere.

Δv_0 = impulse required for the launch from the low-Earth orbit to Venus.

Δv_{10} = impulse required for the manoeuvre to break into the near-Venus orbit.

Δv_{sep} = separation impulse value, km/s.

$\Delta v_{1\Sigma}$ = total cost of the characteristic velocity for orbital operations in Venus SOI, km/s.

$\alpha = 2\arcsin\dfrac{1}{1+r_\pi \left(v_\infty^+\right)^2 / \mu_{pl}}$ = angle between $\mathbf{V}_\infty^-$ and $\mathbf{V}_\infty^+$, rad.

$\alpha^* = 2\arcsin\dfrac{1}{1+r_{\pi,\min} \left(v_\infty^+\right)^2 / \mu_{pl}}$ = natural turn angle, rad, $r_{\pi,\min}$, the minimal allowed periapsis radius during the gravity assist is 6,551 km (in this work).

β = the angle determining the periapsis of a real hyperbolic orbit that belongs to the manifold of orbits with the same energy.

χ_1, χ_2 = right ascension and declination of $\mathbf{V}_\infty^+$ in the planetocentric frame., deg

$\varpi = \arccos\dfrac{1}{1+r_\pi \left(v_\infty^+\right)^2 / \mu_{pl}}$ = angular radius of the circle of possible periapsis, rad.

θ = initial entry angle at the Venusian atmosphere (considered at an altitude of 140 km above the Venus surface), deg.

μ_{pl} = gravitational parameter of the planet, [km^3/s^2];

$\mu_\odot = 132\,712\,440\,018\ km^3/s^2$ – gravitational parameter of the Sun.

Ψ = the angle determining the size of the landing circle, which is the set of possible landing points that form when the manifold of approaching hyperbolas, with a constant *orbital energy* intersect with the Venus surface, deg.

κ = angle between the planes of motion of the orbiter and the lander, deg.

ς = half- angle of the cone formed by the field of view of the radar of the lander, deg.

$\left(\delta h_p\right)_{\text{Sec}}$ - the secular variation in the pericentre altitude of the satellite orbit, km.

1. Introduction

The study of Venus has been one of the most important areas of planetary science over the past five decades [1-3]. Moreover, the last interplanetary stations that directly explored the surface of the planet were the *Vega-1* and *-2* spacecraft launched in 1984 [4, 5]. Later, studies of Venus were conducted only from an orbit of its artificial satellite by the *Magellan*, *Akatsuki*, and *Venus Express* missions, as well as from a flyby trajectory by the *BepiColombo* mission during the flight to Mercury [6-8].

Interest in the study of Venus is primarily caused by its geological and atmospheric features [2-5], as well as various hypotheses about the possibility of habitability. The sheer number of publications devoted to this subject demonstrates the intense interest in the search for potential life. Some of the most popular ones are [10-18]. Currently, a number of projects aimed at exploring the internal structure, surface and atmosphere of the planet are being developed by leading space agencies in different countries.

The Venus exploration projects are at different stages of development and are aimed at solving various scientific problems. Specifically, the main goal of the Russian *Venera-D* project is to gain fundamental knowledge about Venus as a planet and to conduct a detailed study of its surface and atmospheric conditions, as well as its climate and weather. The scientific data collected by the mission are expected to be useful for understanding and predicting the future evolution of climate not only on the Earth but also on various exo-planets, most of which, having Earth-like dimensions, are similar to Venus, which thus can be considered as a "representative of exo-planets" in the Solar system. Additionally, the information gathered during the *Venera-D* mission could be used for future Venusian missions aimed at delivering atmospheric and soil samples to the Earth [8, 18].

An important stage in the development of the project is determining the landing site for the lander. The site should be chosen not only on the basis of the ballistic scenario of the mission and the technical realizability of landing but also out of scientific objectives to be achieved. According to [19-29], from the perspective of studying the internal composition of Venus, such areas of surface relief as tesserae and plains may be of primary scientific interest. Additionally, planetary scientists are strongly interested in studying volcanic activity on the planet via orbital and surface studies of areas associated with the formation of young volcanoes [30-31]. However, despite the wide scientific interest in the study of tesserae, the existing technological restrictions require landing on the plains. In [19-24, 26, 29], four main types of flat landforms were identified as scientifically interesting and technically realizable landing sites. These include 1) stratigraphically the oldest plains, 2) stratigraphically the youngest plains, 3) lobed plains, and 4) channel-shaped plains. In the future, a working group will be formed to map the surface and study the scientific benefits of landing on an area of each type. Ensuring safe landing on various parts of the planetary surface, as discussed in [22, 32], also limits the choice of the landing site.

Achieving the scientific goals of the mission is closely related to technical and natural restrictions imposed on the flight to Venus. Until now, the only way to conduct research on the Venusian surface by a lander was to land it directly from the elliptical Earth–Venus transfer trajectory. As a result, the choice of a landing site for the lander was limited by a number of factors, namely, the slow rotation of Venus (the sidereal rotation period is –243.02 Earth days, sign "–" shows the retrograde direction), severe conditions on its surface for device operation, surface relief itself, and other factors [22, 29, 32].

However, with the progress of space technology, as well as the increase in the number of successfully completed Soviet and American missions to Venus, the problem of ensuring the delivery of a lander to a given area of the planet's surface, which was chosen solely due to its scientific value, became very realistic. Various strategies that increase the scientific potential of planetary exploration missions by using the dynamic features of heliocentric spacecraft trajectories have been proposed for the *Venus flagship* mission project (a complex mission profile including vehicles moving towards Venus with high-thrust and gravity assist manoeuvres as well as small low-thrust vehicles) [34] and for the *DAVINCI+* project (double Venus gravity assist associated with radiosonding of the proposed landing site) [44]. In [47-49], a method of transfer to Venus via a gravity assist manoeuvre and resonant orbits* to ensure landing at any site on the surface was proposed. This flight scenario is also considered in this paper. Let us focus on its description in more detail.

It should be noted that in recent studies [50-51], the authors investigated periodic (resonant) orbits in the Sun-Venus system using numerical simulations of the circular restricted three-body problem. Their research provided approximately 37 stable resonant orbit manifolds, either outer or inner families, either within the orbit of Venus or

*

outside it. These findings can serve as a solid foundation for future Venus missions, as well as being important because they provide evidence for the existence of stable orbits and the feasibility of conducting remote studies of Venus.

For Venusian missions involving landing on the surface of a planet, the use of a gravity assists of Venus, which puts the spacecraft on a resonant orbit, providing a subsequent return to the planet and landing at the desired point on the surface, was proposed in [47]. This scenario qualitatively changes the principles of choosing landing sites on the surface of the planet and allows landing in those areas of the surface that have the highest scientific importance.

The sequence of operations for constructing trajectories in this scenario, according to [47], includes the following stages: (I) calculating the trajectory of the spacecraft's flight from the low-Earth orbit to the boundary of the Earth's sphere of influence (SOI); (II) calculating the interplanetary trajectory of the spacecraft flight from the Earth to Venus, implemented by solving the Lambert problem; (III) calculating the gravitational manoeuvre, which consists of determining the parameters of the required *m*:*n* resonant orbit leading the spacecraft to the targeted landing point on the Venus surface; (IV) calculating how many times the spacecraft needs to orbit Venus while moving along this *m*:*n* resonant orbit; (V) calculating the trajectory of the spacecraft inside the Venus SOI from its outer boundary to the boundary of the planet's atmosphere; and (VI) estimating the displacement of the landing point of the lander as a result of its descent in the planet's atmosphere.

Special attention should be given to the stage (V) of the abovementioned technique. Since the developed methods focus primarily on orbital parts, the developed techniques for calculating the abovementioned stage are used. Promising approaches ensuring the safe landing of a lander on Venus' surface can be found in [32], which also assesses the potential risks associated with landing on terrains and strategies for compensating for these risks to ensure a successful landing. Paper [50] considers a method of landing using a manoeuvrable type of lander, which allows control during descent. The authors of [52-54] proposed a variant of a mission to Venus involving entering an intermediate orbit around the planet's satellite with subsequent landing in a given area.

Another important question related to designing the flight trajectory is a choice of the proper ratio *m*/*n* for the resonant orbit. Note that, as in [47], where the best option from the point of view of a simple assessment of the effectiveness of covering the surface of Venus is to use a 1:1 ratio, in this paper, only mentioned ratio will be considered.

In this work, an analysis of flight trajectories to Venus is performed via the above technique within the framework of assumptions for a reference resonant orbit. In contrast to previous studies, the purpose of the current one is to consider a specific scenario for a flight to Venus including an orbiter and a lander while paying special attention to analysing the requirements for the orbiter's orbit since, in the proposed assumption, these factors influence the choice of a landing site.

Two stages of analysis are considered: 1) analysis of the requirements for an orbit of the orbiter beginning from technical specifications and developing up to their mathematical interpretation, and 2) use of the resulting dependencies for further calculation of possible landing areas for the lander. For the second stage, a comparison of the landing areas covered in the classic (i.e., direct flight) and gravity-assisted approaches is made, and the results are presented in coloured maps.

The results of the analysis showed that the proposed flight scheme, as described in [47-49], provides advantages over classical approaches, even if the choice of a landing site is limited by the requirements for the orbiter's nominal orbit.

2. Material and methods

In this section, we focus on the Earth-to-Venus flight trajectory within the context of the scenario described above. The flight trajectory is calculated via the patched-conic approximation method [55-58]. In this method, the trajectory is divided into three sections: two planetocentric ones and a heliocentric one. In each of these sections, the trajectory is determined by a solution of the corresponding Lambert problem. The trajectory on the heliocentric section between the Earth and Venus can also be determined by the solution of the Lambert problem; methods for solving this problem can be found in various works on astrodynamics, for example, in [58-62].

The calculation of the spacecraft trajectory within the planets' SOI is performed according to the algorithm given in [59]. The initial data for this calculation is the vector of the asymptotic velocity as well as the known inclination and pericenter radius of the hyperbolic trajectory of the spacecraft. The algorithm based on those data is presented in Appendix A1.

The *V*-infinity globe method [62-68] is used to connect the trajectory parts of the Earth-Venus and Venus-Venus transfers, along with a gravity assist arc, considering the latter to be impulseless. Further calculations of the trajectory that ensure the delivery of the lander to the selected site on the planetary surface are performed via the method described in [48], in which the $\mathbf{v}_{\infty}^{+}$ is connected to the landing site in a conical model. Based on [48], where the general

algorithm of using gravity assist with the subsequent transfer to periodic heliocentric orbits was developed, the scheme in Fig. 1 was drawn.

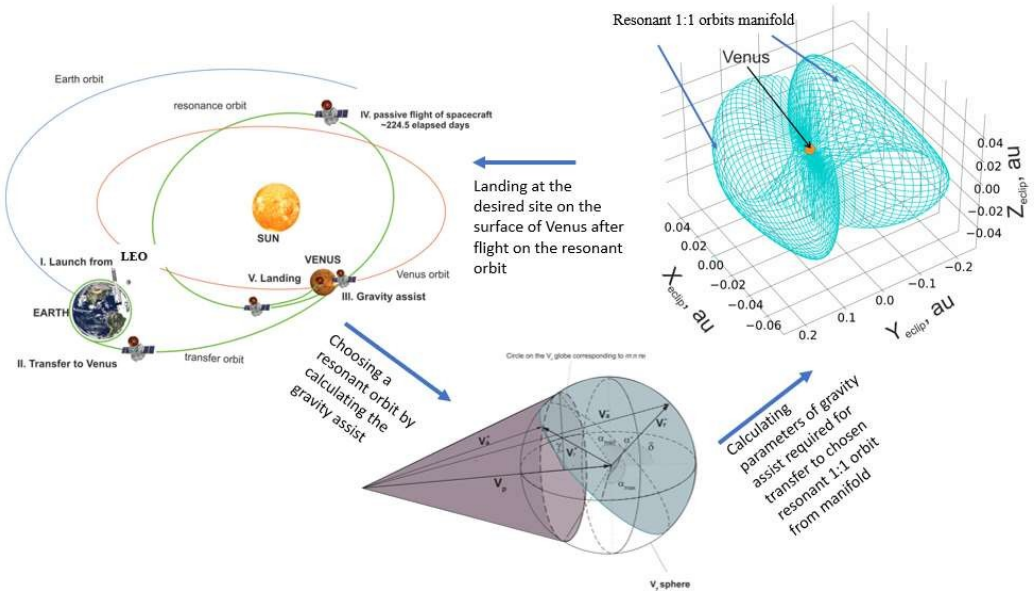

Figure 1. A general scheme showing the idea behind the method in use. This diagram graphically represents the process of calculating the gravity assist parameters in the first case; in the second case, it shows the selection of the required orbits from the presented manifolds to find the trajectory leading to the desired landing site.

In Fig. 1, a brief description of the proposed technique is presented. The key factor in determining the lander's final position is the ability to transit the spacecraft to the desired resonant orbit, and then to the target location. This is made possible by maintaining the asymptotic velocity achieved during the flyby phase, which remains constant in the planet-centered frame. Particularly, all potential landing sites are located on a circle centered at the point where the asymptotic velocity intersects the Venus surface, as described in [47].

Notably, only those resonant trajectories that are reachable through a passive (impulseless) gravity assist manoeuvre around Venus are considered. This can be easily explained by considering the impulse $\Delta v_n = 2\left\|\mathbf{v}_\infty^+\right\|\sin\frac{1}{2}\left(\alpha^* - \alpha\right)$ required for compensating for the difference $|\alpha^* - \alpha|$ between the allowed and the required rotation angles. It can be easily estimated that the impulse required to compensate for a 1-degree difference in trajectory with $C_3 = 9\,km^2/s^2$ is $\Delta v_n \approx 101\ \ m/s$. In these cases, active manoeuvres seem to be highly ineffective in the considered scenarios. Therefore, trajectories that require additional impulses are excluded from analysis.

Another point to note in the above paragraph is that the Oberth manoeuvre, which is the impulse near the periapsis during a planet's flyby, is not taken into account either. This is because, in general, spacecraft approaching Venus have sufficient velocity to allow Venus gravity to decrease their heliocentric velocity and achieve the required value.

The impact of the orbiter's technical constraints on the attainable landing area on the Venus surface can be assessed by dividing the entire set of possible landing sites, which are calculated without considering these constraints, into a finite number of landing points, which are then transformed into a set of planet-centric vectors. The same operation is performed for orbital pericenters, producing a finite set of radius vectors. Then, each pericentric vector is transferred into the set of Keplerian orbital elements, each of them is evaluated for compliance with every given constraint. Finally, it is compared with the corresponding radial vectors of the desired landing point. For apiece landing point, a set of orbits with the same asymptotic velocity must be checked. This procedure is both feasible and practically implementable, requiring minimal computing resources because of the preliminary analysis that can be performed for Keplerian elements.

Therefore, it is necessary to further analyse the most common constraints on the operation of a planetary orbiter to apply them to practical examples for future missions.

1. Analysis of the requirements for the orbiter's nominal orbit

Let us delve into the implementation of the trajectory design methodology for a spacecraft mission to Venus, as outlined in the introductory section of the paper [45]. This mission stands out because of its utilization of a dedicated lander and an orbiter, both of which contribute to the comprehensive exploration of Venus. The inclusion of an orbiter necessitates specific requirements for its working orbit, introducing additional constraints on the landing locations of the lander. This similarity to previous considerations regarding other factors, such as maximum overload and angle of re-entry, makes this approach similar to that previously explored.

To date, there exists only one known mission with plans to implement a similar architecture, namely, *Venera-D*. Therefore, in our analysis, we consider the currently accepted missions as constraints within the project scenario. Each constraint is examined individually, with particular attention given to the duration of the ballistic lifetime of the orbiter.

The design of the spacecraft's trajectory within the scope of the *Venera-D* mission involves the stage of separation of the orbiter from the lander 1-3 days before approaching Venus [69]. The orbiter subsequently breaks into a near-Venus orbit, with its pericentre located at an altitude of 500 km [1, 7]. Building on the aforementioned framework, it is possible to conceptualize a mission trajectory to Venus that involves the decoupling of a spacecraft comprising an orbiter and a lander, the mentioned one is depicted in Fig. 2.

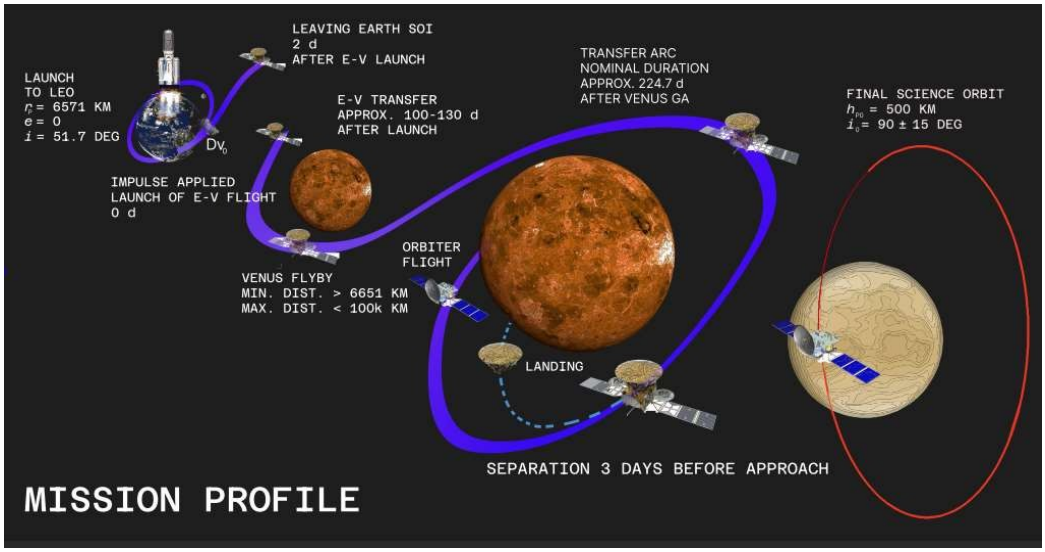

Figure 2. Scheme of spacecraft flight under the scenario proposed in [48], modified to consider orbiter operations in the flight scheme.

Among the space missions to Venus which are currently under of development, *Venera-D* presents a unique opportunity to study the planet. It uses a lander, an orbiter, and an aerial platform to investigate the long-term evolution of the middle atmosphere. This mission configuration, which is based on the requirements formulated in [1, 6 and 69], is a great example for studying the application of the method developed in [47-49]. By applying this method to missions, this paper studies how the constraints put on the orbiter influence the possible areas for landing a lander on the planet's surface.

The list of requirements for the orbiter is provided below, according to [69]:

[1] The cost of the characteristic velocity for the orbiter to enter a near-Venus orbit (braking impulse) is no more than 1700 m/s.
[2] Ensuring mutual radio visibility between the lander and orbiter at all stages of descent and for at least 180 minutes after landing.
[3] The duration of existence of the orbiter in the orbit (ballistic lifetime) is at least 8 years.
[4] The duration of the shadow areas (eclipses) should not exceed 60 minutes.

In the section below, the above requirements will be thoroughly analyzed, and final constraints on the orbiter will be presented.

2.1 Braking impulse

The spacecraft transfer from the hyperbolic approach trajectory to the orbit of a satellite of Venus occurs as a result of a capture manoeuvre. The impulse required for such a manoeuvre can be calculated according to [55, 65]:

$$\Delta v_{10} = \sqrt{\frac{2\mu_{pl}}{r_\pi} + v_\infty{}^2} - \sqrt{2\mu_{pl}\left(\frac{1}{r_\pi} - \frac{1}{2a_0}\right)}, \quad (1)$$

Let us perform the analysis for the case of orbit braking from an incoming hyperbolic trajectory, with an asymptotic approach velocity in the range $3 \le v_\infty \le 5$ (km/s). The results of calculating the impulse needed for orbit entry as a function of the period of the final orbit are given in Table 2.

It can be seen from the data given in Table 2 that the minimum impulse is attained at the shortest distance from the centre of the planet, as deduced from (1). Drawing on the experiences of previous missions such as the *Venera* series and *Venus Express*, it can be inferred that the braking manoeuvre occurs at an altitude of approximately 500 km above the mean distance to the surface of Venus, assuming that the surface of the planet can be approximated as a sphere with a radius of 6,051 km on average. Consequently, the perigee of the nominal orbit must always be considered at a height of 6,551 km.

Table 2. Costs of the characteristic velocity for the transition to the orbit of an artificial satellite of Venus depending on the period of the final orbit. The radius of the pericentre of the final orbit is located at an altitude of 500 km.

Period of the near-Venus orbit, h	Semimajor axis, km	Eccentricity	Δv_{10}, km/s (3 km/s)	Δv_{10}, km/s (5 km/s)
24	39,457	0.834	0.864	1.607
48	62,634	0.899	0.706	1.449
72	82,073	0.924	0.643	1.385
96 (unstable)	99,425	0.938	0.607	1.350
120 (unstable)	115,372	0.947	0.584	1.327

According to the experience of the currently operated missions, particularly *Venus Express* [3], as well as the draft scenario of the *Venera-D* mission [69] and the research conducted in this paper (Table 2), only 24 hr orbits near Venus are considered.

2.2 Mutual radio visibility between the orbiter and the lander

The constraint on the duration of mutual radio visibility between the orbiter and the lander ($T_1 > 180\ min.$) was taken into account by an additional solution to the following problem. The position of the lander was fixed at the moment of re-entry, and the position of the orbiter was moved to the pericentre of its hesperocentric orbit. It was assumed that the field of view of the radar of the lander formed a cone with a half-solution angle ς and an axis passing against the planetocentric distance connecting the position of the lander and the center of Venus. The solution of the problem consists of finding the maximum of the functional characterizing the duration of the radio communication session between the orbiter and the lander ($T_1 \to max$), on the interval of angles between the planes of motion of the orbiter and the lander ($\kappa \in (0°; 360°)$). According to the numerical evaluation made by the gradient method, $\kappa = 180°$, $\varsigma \le 90$ (i.e., when the transmitter antenna located on the landing vehicle is assumed to be omnidirectional). For the constraint adopted in *Venera-D* ($T_1 > 180\ min$) taking $\varsigma = 90$, the constraint on T_1 is fulfilled at $\kappa = 180° \pm 15°$. The solution to the problem of determining the duration of the radiovisibility interval is given in Appendix A.2.

2.3 Orbiter lifetime

Analysis of the orbital motion of a satellite in a highly elliptical orbit around a planet can be performed via analytical, semianalytical, and numerical methods. The analytical and semianalytical methods include the classical perturbation theory developed by M.L. Lidov (Kozai–Lidov theory of satellite motion) [72, 73], which is based on the spatial elliptic three-body problem in the Hill formulation for satellites. For numerical analyses, the approaches described in Battin [74], Vallado [70], and Bate [75] can be used. The basis of these approaches is the numerical

integration of the equations of motion; the difference lies in the different types of equations that can be used for this analysis.

Let us consider the most commonly used model of spacecraft motion in the form of a second-order vector differential equation written relative to the radius vector of the spacecraft:

$$\ddot{\mathbf{r}} = -\frac{\mu_{pl}}{r^2}\cdot\frac{\mathbf{r}}{r} + \sum_{j=1}\boldsymbol{\alpha}_j. \tag{2}$$

This model can be considerably simplified, for example, if the accuracy requirements at the initial design stage can be slightly relaxed. Let us perform a preliminary analysis of the values of perturbing accelerations acting on the satellite orbiting Venus.

Consider the following perturbations, with a designation of the corresponding curve in the Figure 4 given in parentheses:

1. Gravitational pull:
   - The Sun (SUN);
   - Jupiter (JUP);
   - Earth–Moon Systems (EARTH).
2. Relativistic effect (accounting for Schwarzschild functions, Lens-Tirring precession effect) (RELAT);
3. The gravitational field of Venus (64x64 harmonics) (GRAVITY);
4. The cumulative effect of the above perturbations (ALL).

The expressions used to numerically estimate the above accelerations on the satellite can be fully found in Battin and Bate et al. [71-72]. Figure 3 shows acceleration magnitudes calculated using the expressions from the reference and plotted on a logarithmic scale along both the horizontal and vertical axes.

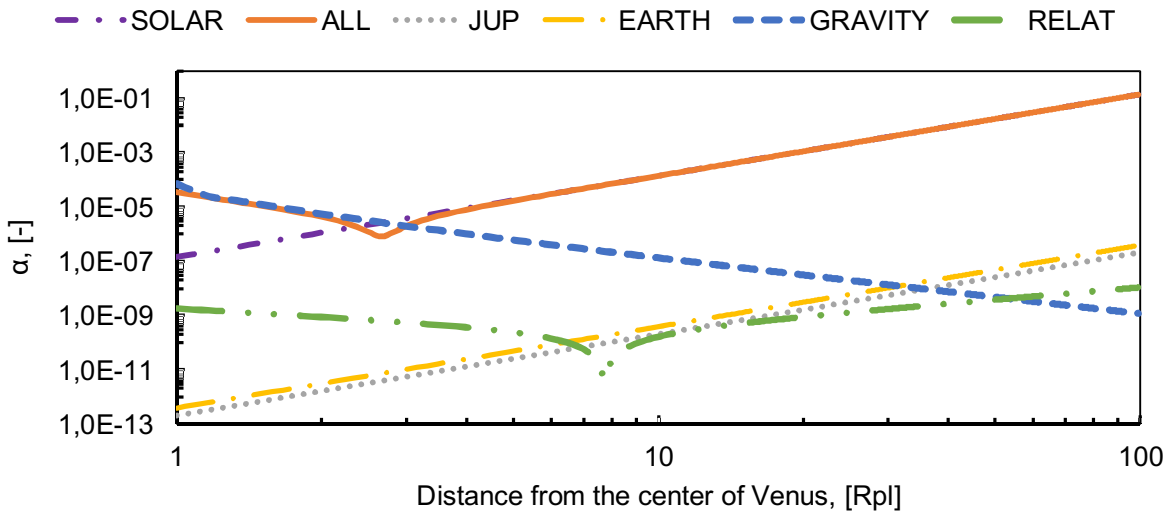

Figure 3. Perturbative acceleration of spacecraft motion vs. the distance from the Venus center of mass on a logarithmic scale

The analysis of disturbing influences of various nature shows that at a distance not exceeding 100 thousand km, it is enough to consider only the gravitational influence of the Sun.

Since the trajectory of a satellite experiences the greatest perturbation under solar gravity, one can use this trajectory for simplified analysis. A model for calculating the motion of an orbiter is well known as Cowell's third-body perturbation [72, 76]:

$$\ddot{\mathbf{r}} = -\frac{\mu_{pl}}{r^2}\frac{\mathbf{r}}{r} + \left(\frac{\mu_{\odot}(\mathbf{r}_{\odot}-\mathbf{r})}{r_{10}^3} - \frac{\mu_{\odot}\mathbf{r}_{\odot}}{r_{\odot}^3}\right). \tag{3}$$

The theory of motion [72, 76] provides us with the dependence of the secular evolution of the pericenter radius on the inclination and the argument of the periapsis with respect to the perturbing body:

$$\left(\delta h_p\right)_{\text{Sec}} = -\frac{15}{4}\pi \frac{\mu_1}{\mu_0}\left(\frac{a}{r_1}\right)^3 ae\sqrt{1-e^2}\sin^2 i \sin 2\omega\,. \tag{4}$$

The orbital plane of the perturbing body is taken as the basic plane, where $a = a_0, e = e_0, i = i_0, \omega = \omega_0$ represent the initial values of the satellite orbital elements.

The above equalities (4) do not depend on the longitude of the satellite's ascending node. Thus, studying the satellite lifetime will be sufficient to change the initial argument of the pericentre and orbital inclination at other fixed orbital parameters, $a_0 = 39456$ km, $e_0 = 0{,}8339$, $\Omega_0 = 0$ deg. Let us estimate the orbiter existence time via numerical simulation of orbiter motion within the framework of model (3) by changing the initial values of ω_0 and i_0 at a fixed pericentre altitude (500 km) and orbital period (24 hr). The calculation results are shown in Fig. 5 for different values of ω_0 and i_0.

From Fig. 5, one can clearly distinguish four regions in ω_0 and i_0 corresponding to long (more than 5 years) and short periods of existence. Let us allocate those regions on ω_0, corresponding to the high value of the ballistic lifetime of the satellite (given for the value $i_0 = 90$ deg):

$$\begin{cases} 90^o < \omega_0 < 180^o \\ 270^o < \omega_0 < 360^o \end{cases}, \tag{5}$$

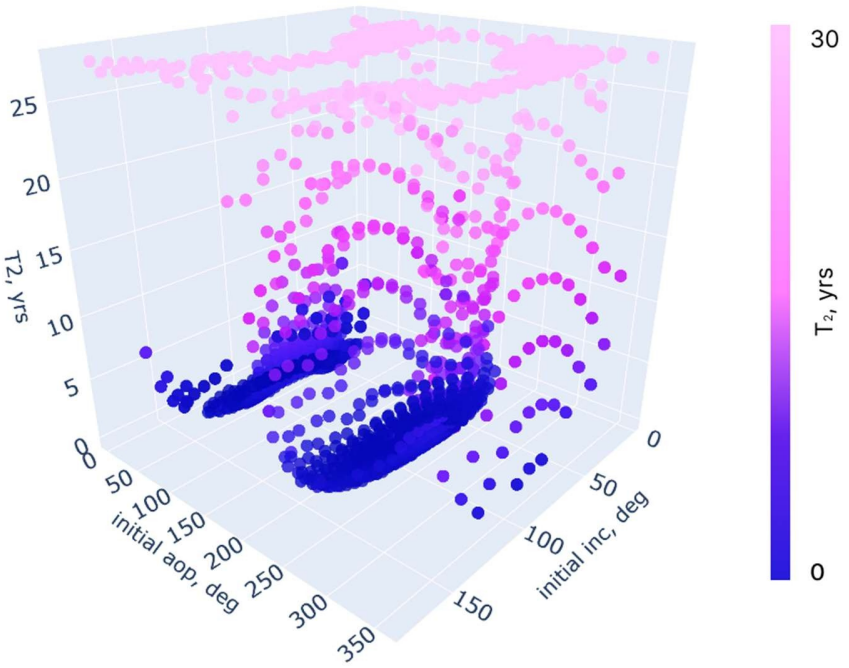

Figure 5. T_2 vs. ω_0 and i_0. *Note* that the color highlights the ballistic lifetime (T_2)

Note that the results obtained for the duration of the ballistic lifetime of the orbiter in a 24 hr highly elliptical orbit from the initial value of ω fully correspond to the regions of increasing periapsis altitude under perturbations from external bodies [76].

3. Results

3.1 Direct flight scenario for the 2029 and 2031 launch windows

Let us first consider the classical approach, for example, the mission plans for *Venera-D*, which are sheduled to be launched between 2029 – 2031 yrs, according to [69]. Based on this paper, let us use the combination of $\Delta v_0 + \Delta v_{10}$ discussed in [49] for minimizing characteristic velocity costs in the problem of trajectory optimization. Let us plot the dependences of the launches Δv_0 and Δv_{10} on the date of launch to Venus for both launch windows (Fig. 6).

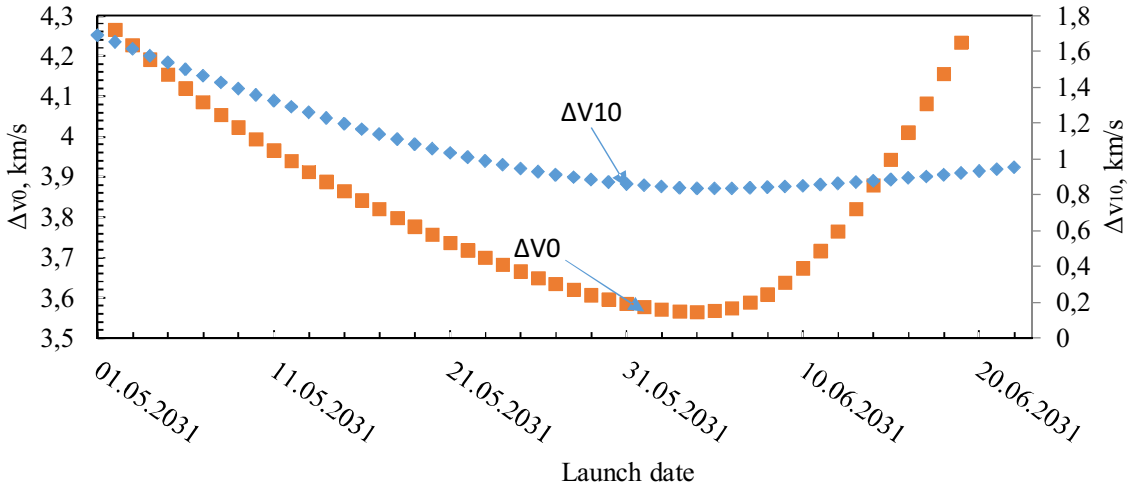

Figure 6. Dependence of the Δv_0† required for launching a mission to Venus on the launch date and arrival date for missions launched in 2029 and 2031; the required braking impulse Δv_{10} for entering a 24 hr period orbit.

According to the conclusions of the previous section, let us analyse the attainable landing points, taking as a reference the 24 hr near-Venusian orbit, i.e., an orbit with a_0 =39456 km and e_0 = 0.8339. The inclination of the orbit is a free parameter, although in more recent scientific studies, the nominal inclination should be close to polar, i.e., i_0 =90°, as in [69]. The initial values of the longitude of the ascending node and the pericentre argument are determined by the date of the spacecraft approach Venus according to Appendix A.1.

The attainable landing regions obtained in the direct flight scenario with and without orbiter constraints are plotted in Fig. 7.

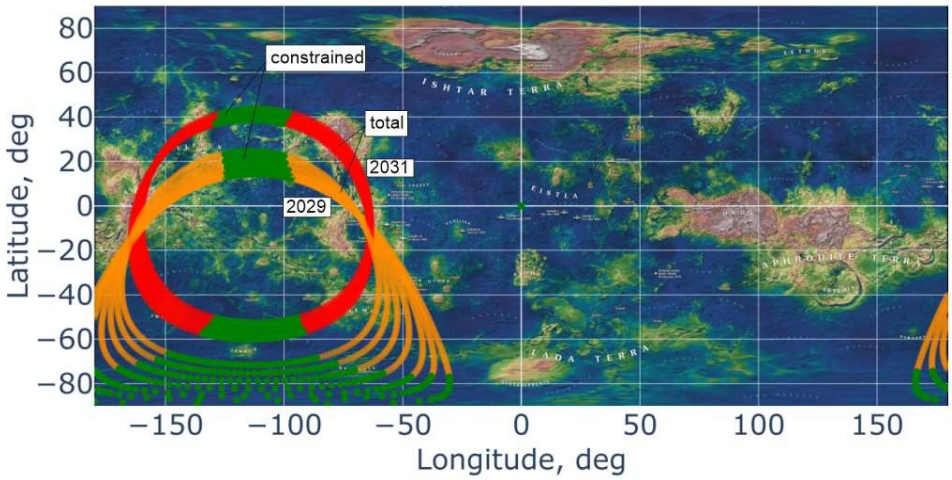

Figure 7. Total landing area (red–orange) constructed without considering orbiter analysis; (green) area trimmed according to orbiter requirements.

The presence of the orbiter greatly restricts the attainable landing areas, primarily due to the requirement for a ballistic lifetime. Although the strict constraint on radio visibility also makes landing in the plotted red–orange area on any launch/arrival date within the considered launch window impossible.

† Calculated as the difference between required hyperbolic velocity to leave the Earth sphere of influence and velocity of the spacecraft on circle parking orbit with parameters that is altitude 200 km and inclination 51.6 deg.

3.2 Determination of attainable landing areas in the lander/orbiter mission scenario

Let us provide an example of calculating the attainable landing areas on the surface of Venus, considering the orbiter requirements for the launch windows in 2031 (Table 3), and compare them with a direct flight on the same launch dates. Notice that trajectories were optimized taken into account the criteria provided above.

In Fig. 8*a*, the manifolds of the resonant 1:1 orbits are drawn using the method described in [49], based on the data from Table 3 for a launch date in 2031.

Table 3. Parameters of flight trajectories to Venus in 2031.

Parameter	Unit.	Parameter value	
Launch date, dd.mm.yyyy (UTC)	-	12.06.2031 12:00	Direct flight
β^{0*}	deg	41.66 (prograde)/ 138.33 (retrograde)	
Δv_0 $(C_3)^E$**	km/s $(km/s)^2$	3.79 (14.38)	
$v_{\infty 0}^0$ $(\alpha_{\infty 0}^0, \delta_{\infty 0}^0)$	km/s, (deg, deg)	3.89 (121.28, -20.86)	
Flyby date, dd.mm.yyyy (UTC)	-	10.10.2031 22:36	
SEV	deg	153.75	
v_∞^- $(\alpha_\infty^-, \delta_\infty^-)$	km/s	3.01 (141.56, -4.36)	
Range of permissible γ_1 [47]	deg	$0, 360$ (Φ_1 =92.45)	Resonant orbit flight
Landing date, dd.mm.yyyy (UTC)	-	22.05.2031 15:24	
SEV	deg	172.94	
v_∞^+	km/s	3.01	

Note: Parameters are set in reference to the ecliptic heliocentric coordinate system for the J2000 epoch; parameters of the low-Earth orbit from which the spacecraft is launched are assumed to be a radius of 6571 km and an inclination of 51.6° to the Earth J2000 equator; SEV - Sun–Earth–Venus angle; * - azimuth value for the launch hyperbolic trajectories to Venus. ** - value of the orbital energy of the spacecraft at the boundary of the Earth's SOI.

The attainable landing areas based on data in Table 3 considering possible launches at 12.06.2031 are plotted in Fig. 8*b*, respectively. The attainable landing area in Fig. 8*b* is the total number of cyan points for 2029 and pink points for 2031 points on the Venus surface map calculated via the approach discussed in Section 2. Only the areas that meet the requirements for landing are considered when determining the attainable landing region.

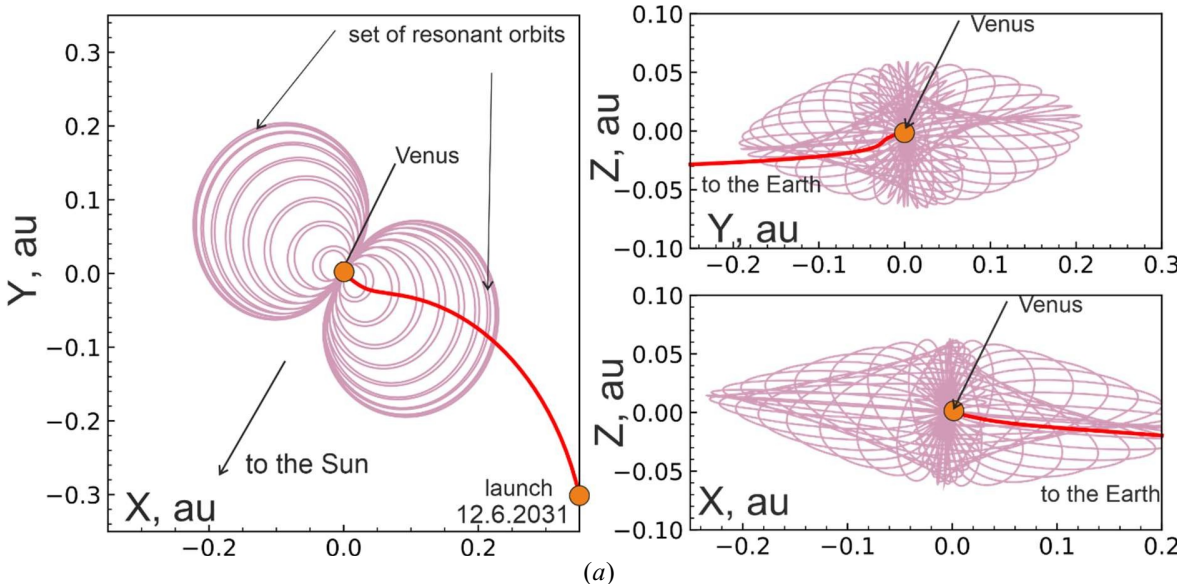

(*a*)

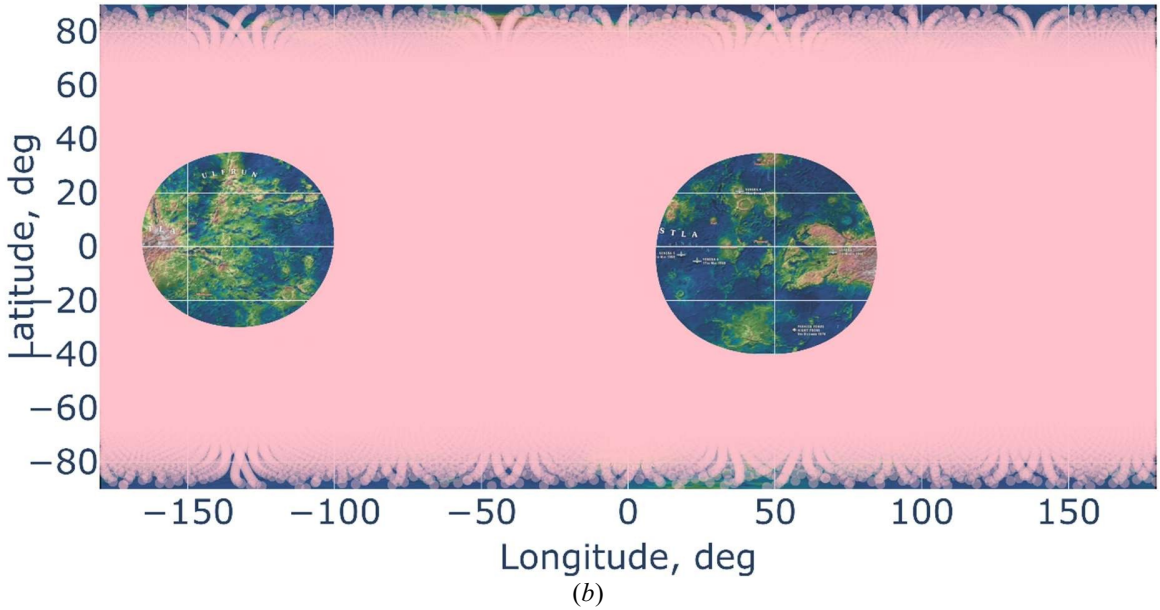

(*b*)

Figure 8. (*a*) Stage of gravity assist operation and resonant orbit selection; each of the orbits of the drawn manifold is accessible to transit to using gravity assist of Venus, the resonant orbits 1:1 manifold plotted for $v_\infty^- = 3.01\ km/s$ at approach date of Venus at 10.10.2031. *Notice: XYZ* is the ecliptic J2000 coordinate system centred at Venus. (*b*) Attainable landing areas at a -12 deg entry angle without considering satellite orbit constraints for a launch date of 12.06.2031 (within the 2031 launch window).

A comparison of Figures 7 and 8*b* reveals that the total landing area obtained via the method mentioned in Section 2 provides more attainable landing areas in all the scenarios. This occurs because the use of gravity assist provides us with more opportunities since there are manifold resonant 1:1 orbits in which every chosen orbit leads to different parts of Venus at the planet's second approach. Therefore, with a wider choice between landing sites, the primer role of gravity assist is to allow impulse-free transition of spacecraft to the required orbit.

3.3 Attainable landing areas in orbiter-lander scenario

Let us calculate the attainable landing areas for the scenario when orbiter operations are included (see Fig 14) using previous data from Table 3. On the basis of the analysis conducted in the previous section, let us review the main constraints for the orbiter:

(1) The basic parameters of the spacecraft orbit are as follows: $a_0 = 39456\ km$, $e_0 = 0.8339$.

(2) Ballistic lifetime with little regard to inclination is satisfied when:

$$\begin{cases} 90^o \le \omega_0 \le 180^o \\ 270^o \le \omega_0 \le 360^o \end{cases}.$$

(3) The radio visibility constraint is completely achieved when $\kappa = 180^\circ$.

(4) Eclipse duration constraints are counted via diagrams shown in sec. 2 (see Fig. 8 as an example). By using those diagrams for a given initial inclination of the satellite orbit and initial ω_0, Ω_0, the eclipse duration T_3 is determined and compared with the allowable duration. If the condition is satisfied, then the corresponding landing point is accepted.

Additionally, an analysis has been conducted in which, for several scientific reasons, the initial inclination may be constrained. In general, for Venus study, the primary interest lies in polar or subpolar orbits to study atmospheric variation at higher latitudes [1-4]. Therefore, taking $i_0 = 90$ deg as a baseline, the following ranges of inclination have been considered: (a.) $0^\circ \le i_0 \le 180^\circ$, (b.) $45^\circ \le i_0 \le 135^\circ$, (c.) $75^\circ \le i_0 \le 105^\circ$, (d.) $i_0 = 90^\circ \pm 1^\circ$.

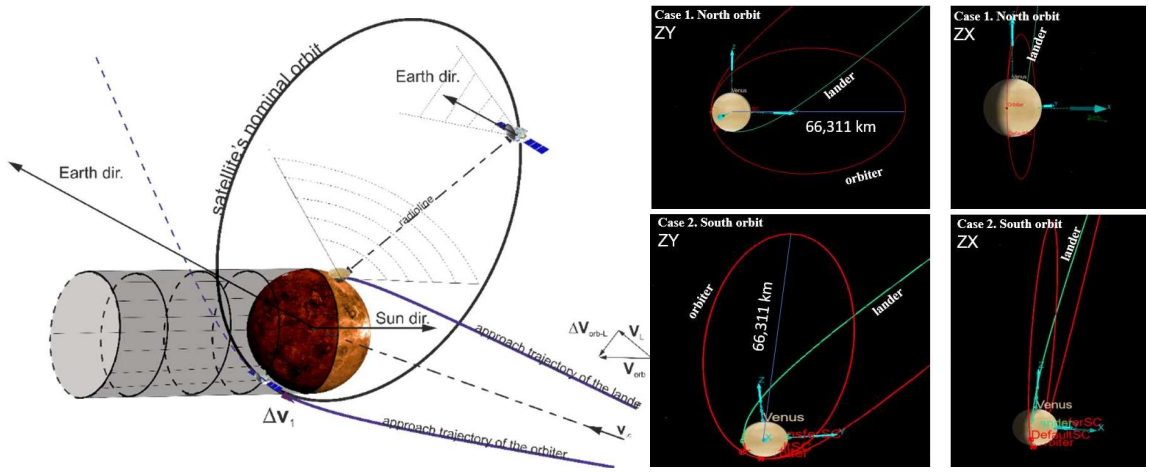

Figure 9. (a) Scheme of the spacecraft near-Venus operations at the stage of the Venus approach based on the [69]; (b) Example of two types of polar orbits with two different ω_0; case 1 – ω_0=180 deg, case 2 – ω_0 = 92 deg. *Note*: All designations other than white in the images have a technical meaning and do not affect the description of the image.

Let us plot attainable landing areas, taking into account the requirements for the orbiter (see Fig. 15-16).

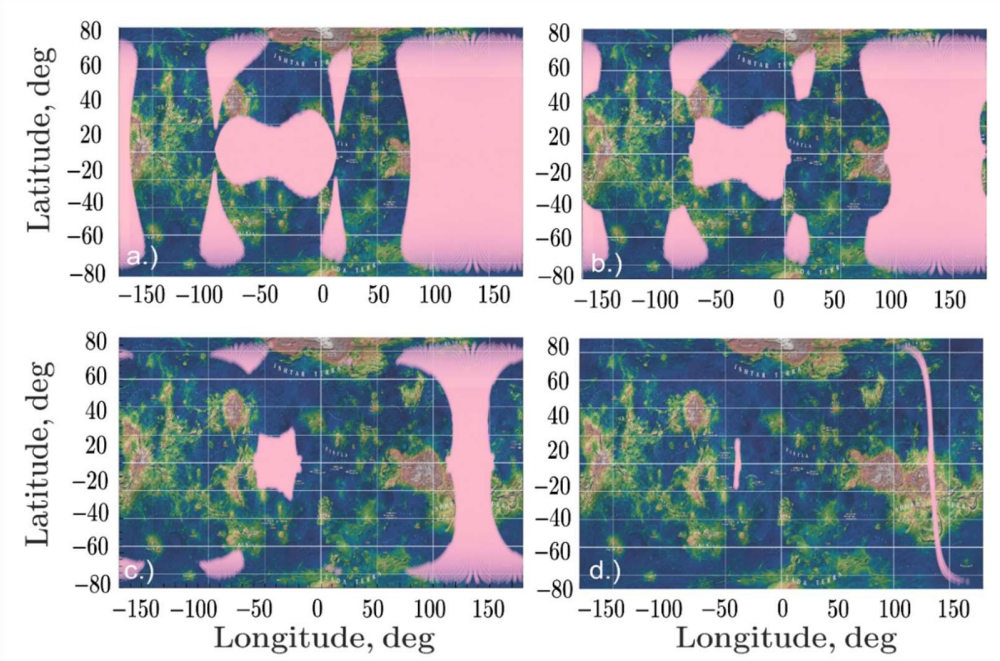

Figure 10 Attainable landing areas at a –12 deg atmosphere entry angle when constraints are considered $T_1 + T_2 + T_3$. (*a*) $0^\circ \le i_0 \le 180^\circ$, (*b*) $45^\circ \le i_0 \le 135^\circ$ (*c*) $75^\circ \le i_0 \le 105^\circ$; (*d*) $i_0 = 90^\circ \pm 1^\circ$ for the launch date 2.06.2031.

In Figs. 10 (cases (a), (b), and (c)), one can see that the application of constraints to the satellite's orbit leads to a decrease in the coverage of the Venus surface by potential landing sites. The main reason for this is orbital inclination constraints, which reduce the number of attainable landing areas, making some previously accessible areas unreachable even with the aid of gravity. Therefore, cases (*a-c*) account for approximately 40 to 60% of original coverage. In case (*d*) of Figs 10, approximately 5% of the initial coverage remains accessible, compared to Fig. 8*b*.

However, it should be noted that in the case of significant tightening of requirements to the orbiter, the landing areas (Fig. 15, 16) plotted for chosen launch date (10.11.2029 and 12.06.2031) are quite reduced (down to 40–50% of the initial Fig. 8*b*) in comparison with the case in which no orbit restrictions are imposed, the obtained attainable landing area is still much larger than that in the case of the direct flight. Recall that in the framework of the direct flight, the attainable landing area is limited only by the circle which the landing points belong to (no more than 5% of the entire surface of Venus within the entire launch window).

Moreover, when analysing the restrictions on T_2 and T_3, some contradiction is observed in the sense that T_2 is convinced of orbits with a small inclination to the planet's orbit, whereas the smallest values of T_3 are provided by orbits of large inclination localizing in the subpolar regions, forming two maxima shown on the diagram Ω_0, ω_0 (see Fig. 8). Thus, the combined effect of these two constraints and the presence of a strict relationship between the orbiter and the lander orbits (κ = 180 deg) leads to a reduction in the attainable landing regions.

6. Conclusions

The study analyses the use of a technique for constructing a flight trajectory to Venus via a gravity assist manoeuvre and resonant orbits to ensure that the vehicle lands in a specified region on the surface of Venus.

As a result of the evaluation of the influence of the pericentre evolution of the orbiter under the influence of the gravity of external celestial bodies in relation to Venus, it was established that there are regions in the space of the parameters ω_0 and i_0, for which the requirement for a long (more than 8 years) ballistic lifetime of the orbiter is provided.

When the total attainable landing area for a landing vehicle is calculated, the overall impact of applying all the constraints for a near-Venusian orbit satellite leads to a reduction in the attainable landing areas (by more than 30–40%). However, combination of the individual areas obtained for each launch/landing dates within the entire launch window makes it possible to virtually compensate for this negative effect. A similar effect can also be achieved by relaxing some of the restrictions, for example, by shortening the duration of radio visibility.

Appendix A1. Determination of orbit parameters from known asymptotic velocity projections

Initial data for calculation:

- $\mathbf{v}_\infty = v_\infty \left[\cos\chi_1 \cos\chi_2 \quad \sin\chi_1 \cos\chi_2 \quad \sin\chi_2\right]^T$, the projections of the asymptotic velocity vector are given in the ecliptic coordinate system with the center in the center of masses of Venus;
- i_0, orbital inclination, rad;
- r_π, pericentre radius, km.

Calculation:

1. Let us define

$$\varpi = \arccos\left(-\frac{1}{1+r_\pi v_\infty^2/\mu_1}\right).$$

2. The energy parameters of the orbit can be determined as:

- Semimajor axis:

$$a_0 = -\frac{\mu_1}{v_\infty^2}.$$

- Eccentricity:

$$e_0 = 1 + \frac{r_\pi v_\infty^2}{\mu_1}.$$

3. Ω_0, ω_0 can be determined as follows:

- To determine the remaining elements of the orbit, we introduce the parameter β, the geometric meaning of which can be expressed as the angle between the projection of the pericenter radius on the plane orthogonal to the vector $\mathbf{v}_\infty$. Let us also define coefficients

$$A_1 = r_\pi v_{\infty,y}; A_2 = r_\pi v_{\infty,x}; A_3 = r_\pi v_\infty \sin\varpi;$$

$$\xi = \frac{-A_1 \sin\chi_1 \sin\varpi - A_2 \cos\chi_1 \sin\varpi}{-A_3 \cos i + A_2 \cos\beta \sin\chi_2 \sin\varphi_1 - A_1 \cos\varpi \sin\chi_2 \cos\chi_1},$$

$$\zeta = \frac{A_1 \cos\chi_1 \cos\chi_2 \sin\varpi - A_2 \sin\chi_1 \cos\chi_2 \sin\varpi}{-A_3 \cos i_0 + A_2 \cos\varpi \sin\chi_2 \sin\chi_1 - A_1 \cos\varpi \sin\chi_2 \cos\chi_1},$$

$$C_1 = -\frac{2\xi}{\zeta+1}, \; C_2 = -\frac{\zeta-1}{\zeta+1}..$$

One can obtain the equation

$$\beta^2 + C_1\beta + C_2 = 0,$$

whence it readily follows

$$\begin{cases} \frac{\beta_1}{2} = \arctan\left[-\frac{1}{2}\left(C_1 - \sqrt{C_1^2 - 4C_2}\right)\right], \; i_0 < \pi/2 \\ \frac{\beta_2}{2} = \arctan\left[-\frac{1}{2}\left(C_1 + \sqrt{C_1^2 - 4C_2}\right)\right], \; i_0 > \pi/2 \end{cases}.$$

- Let us determine the radius of the pericentre $\mathbf{r}_\pi$ via the following method [71]:

$$\mathbf{r}_\pi = r_\pi \begin{bmatrix} \cos\widetilde{\chi}_1\left(\sin\varpi\cos\beta\cos\widetilde{\chi}_2 + \cos\varpi\sin\widetilde{\chi}_1\right) - \sin\widetilde{\chi}_1\sin\varpi\sin\beta \\ \sin\widetilde{\chi}_1\left(\sin\varpi\cos\beta\cos\widetilde{\chi}_2 + \cos\varpi\sin\widetilde{\chi}_1\right) + \sin\widetilde{\chi}_1\sin\varpi\sin\beta \\ \cos\widetilde{\chi}_2\cos\varpi - \sin\varpi\cos\beta\sin\widetilde{\chi}_2 \end{bmatrix},$$

where $\widetilde{\chi}_1 = \chi_1$, $\widetilde{\chi}_2 = \chi_2 + \pi/2$.

- The longitude of the ascending node is as follows:

$$\tan\Omega_0 = -\frac{\sin\chi_1\cos\beta + \sin\beta\sin\chi_2\cos\chi_1}{\sin\beta\sin\chi_2\sin\chi_1 - \cos\chi_1\cos\chi_2}.$$

Obviously, the obtained value can be within the range:

$$0 \le \Omega_0 \le 2\pi .$$

- Argument of periapsis:

Let us define the vector of orbit nodes:

$$\mathbf{k} = \begin{bmatrix}\cos\Omega_0 & \sin\Omega_0 & 0\end{bmatrix}^T.$$

Let us introduce a variable:

$$\rho_1 = \sqrt{\frac{1}{1-\cos^2\chi_2\sin^2\beta}}.$$

After the transformations, we obtain:

$$\cos\omega_0 = \frac{\mathbf{r}_\pi\mathbf{k}}{r_\pi} = \rho_1\left(\sin\chi_2\sin\varpi + \cos\beta\cos\chi_2\sin\chi_1\right).$$

Obviously, on the basis of the geometry of the problem, the argument of the pericentre will be bounded and will be within the following limits:

$$\chi_2 + \varpi \le \omega_0 \le \arccos\left(\mathbf{v}_\infty/v_\infty \cdot \mathbf{k}\right) + \varpi .$$

References

[1] L. Zasova, N. Ignatiev, O. Korablev et al Venera-D Joint Science Definition Team. – Venera-D: Expanding Our Horizon of Terrestrial Planet Climate and Geology Through the Comprehensive Exploration of Venus. Report of the Venera-D Joint Science Definition Team. Moscow, Space Research Institute of the RAS. 2019. 93 p.
[2] Colin, Lawrence. 1977. “The Exploration of Venus.” Space Science Reviews 20 (3): 249–58.
[3] Glaze, Lori S., Colin F. Wilson, Lydmila V. Zasova, Masato Nakamura, and Sanjay Limaye. 2018. “Future of Venus Research and Exploration.” Space Science Reviews. https://doi.org/10.1007/s11214-018-0528-z.
[4] Limaye, Sanjay S., and James B. Garvin. "Exploring Venus: next generation missions beyond those currently planned." Frontiers in Astronomy and Space Sciences 10 (2023): 1188096.
[5] O’Rourke, Joseph G., et al. "Venus, the planet: introduction to the evolution of Earth’s sister planet." Space Science Reviews 219.1 (2023): 10.
[6] Widemann, Thomas, et al. "Venus evolution through time: key science questions, selected mission concepts and future investigations." Space Science Reviews 219.7 (2023): 56.
[7] The Venera-D concept, scientific exploration of Venus in the post-2025 time/D Senske, L Zasova, T Economou et al.//Planetary Science Vision 2050 Workshop. – 2017. – C.1–2.
[8] Zasova, Ludmila, et al. "Venera-D: expanding our horizon of terrestrial planet climate and geology through the comprehensive exploration of Venus." Venera-D Joint Science Definition Team Final Report, Space Research Institute, Moscow, Russia, pp (2017): 1-93.

[9] Taylor, Fredric W. 2014. The Scientific Exploration of Venus. Cambridge University Press.
[10] D'Incecco, P., J. Filiberto, I. López, D. A. Gorinov, G. Komatsu, A. Martynov, and P. Pisarenko. 2021. "The Young Volcanic Rises on Venus: A Key Scientific Target for Future Orbital and in-Situ Measurements on Venus." Solar System Research 55 (4). https://doi.org/10.1134/S0038094621040031.
[11] D'Incecco, P., et al. "Mount Etna as a terrestrial laboratory to investigate recent volcanic activity on Venus by future missions: A comparison with Idunn Mons, Venus." *Icarus* 411 (2024): 115959.
[12] Ivanov, M. A. 2016. "Discriminant and Factor Analyses as Tools for Comparison of Terrestrial and Venusian Volcanic Rocks." Geochemistry International 54 (1). https://doi.org/10.1134/S0016702916010055.
[13] Ivanov, M. A., L. V. Zasova, M. V. Gerasimov, O. I. Korablev, M. Ya Marov, L. M. Zelenyi, N. I. Ignat'ev, and A. G. Tuchin. 2017. "The Nature of Terrains of Different Types on the Surface of Venus and Selection of Potential Landing Sites for a Descent Probe of the Venera-D Mission." Solar System Research 51 (1). https://doi.org/10.1134/S0038094617010026.
[14] Ivanov, M. A., L. V. Zasova, L. M. Zeleny, M. V. Gerasimov, N. I. Ignatiev, O. I. Korablev, and M. Ya Marov. 2017. "Estimates of Abundance of the Short-Baseline (1-3 Meters) Slopes for Different Venusian Terrains Using Terrestrial Analogues." Solar System Research 51 (2). https://doi.org/10.1134/S0038094617020034.
[15] Ivanov, M A, J W Head, L V Zasova, O.Yu. Sedykh, and A V Simonov. 2021. "Criteria for Venera-D Mission Lander Site Selection." In The Twelth Moscow Solar System Symposium 12 M-S3, 109–12.
[16] Ivanov, M A, L Zasova, and T K P Gregg. 2018. "Venera-D Landing Site Constraints." In The Ninth Moscow Solar System Symposium 9 M-S3, 58–59.
[17] Basilevsky, A. T., M. A. Ivanov, J. W. Head, M. Aittola, and J. Raitala. 2007. "Landing on Venus: Past and Future." Planetary and Space Science 55 (14). https://doi.org/10.1016/j.pss.2007.09.005.
[18] Phosphine gas in the cloud decks of Venus/J. Greaves, A. Richards, W. Bains et al.//Nature Astronomy. – 2021. – V. 5. – №. 7. – P. 655–664.
[19] Greaves, Jane S., Anita M.S. Richards, William Bains, Paul B. Rimmer, Hideo Sagawa, David L. Clements, Sara Seager, et al. 2021. "Phosphine Gas in the Cloud Decks of Venus." Nature Astronomy 5 (7): 655–64. https://doi.org/10.1038/s41550-020-1174-4.
[20] Greaves, Jane S., Anita M.S. Richards, William Bains, Paul B. Rimmer, David L. Clements, Sara Seager, Janusz J. Petkowski, Clara Sousa-Silva, Sukrit Ranjan, and Helen J. Fraser. 2021. "Reply to: No Evidence of Phosphine in the Atmosphere of Venus from Independent Analyses." Nature Astronomy 5 (7): 655–64. https://doi.org/10.1038/s41550-021-01424-x.
[21] Limaye, Sanjay S, Rakesh Mogul, David J Smith, Arif H Ansari, Grzegorz P Słowik, and Parag Vaishampayan. 2018. "Venus' Spectral Signatures and the Potential for Life in the Clouds." Astrobiology 18 (9): 1181–98.
[22] O. R. Kotsyurbenko Search for life on Venus: history of the problem and basic concept. Solar System Research, 2023, Vol. 57, No. 3, pp. 232-247 DOI: 10.31857/S0320930X23030052
[23] Villanueva, G. L., M. Cordiner, P. G.J. Irwin, I. de Pater, B. Butler, M. Gurwell, S. N. Milam, et al. 2021. "No Evidence of Phosphine in the Atmosphere of Venus from Independent Analyses." Nature Astronomy. https://doi.org/10.1038/s41550-021-01422-z.
[24] Venus' spectral signatures and the potential for life in the clouds/S. Limaye, R. Mogul, D. Smith et al.//Astrobiology. – 2018. – V. 18. – № 9. – P. 1181–1198.
[25] No evidence of phosphine in the atmosphere of Venus from independent analyses/Villanueva, G. L., Cordiner, M., Irwin, P. G. et al.//Nature Astronomy. – 2021. – V. 5. – №. 7. – P. 631-635.
[26] De Mol, Maarten L. "Astrobiology in Space: A Comprehensive Look at the Solar System." Life 13.3 (2023): 675.
[27] Gregg, T.K.P. and S.E.H. Sakimoto, 2019, On the significance of Venusian canali, Venera-D Landing Site Selection Workshop, October 2-3, 2019, Moscow, Russia.
[28] Herrick, R.R., D.L. Stahlke and V.L. Sharpton, 2012, Fine-scale Venusian topography from Magellan stereo data, Eos 93(12):125-126.
[29] Izenberg, N.R. and M. Lessis, 2019, APL's Venus Environment Chamber (AVEC) : Initial tests, current and future work, Venera-D Landing Site Selection Workshop, October 2-3, 2019, Moscow, Russia.
[30] Kremic, A.T., B.B. Eppig and C.J. Balcerski, 2019, Glenn Extreme Environment Rig (GEER), Venera-D Landing Site Selection Workshop, October 2-3, 2019, Moscow, Russia.
[31] Rabinovitch, J. and K.M. Stack, 2019, Global characterization of safe landing sites on Venus using Venera panoramas and Magellan radar properties, Venera-D Landing Site Selection Workshop, October 2 - 3, 2019, Moscow, Russia.
[32] Knicely, Joshua JC, et al. "Strategies for safely landing on Venusian tesserae." Planetary and Space Science 228 (2023): 105652.

[33] Zasova, L. V., et al. "Venera-D: A design of an automatic space station for Venus exploration." *Solar System Research* 53 (2019): 506-510.
[34] Venus Flagship Mission Concept: a decadal survey study/P. Beauchamp, M. Gilmore, R. Lynch et al.//IEEE Aerospace Conference. – 2021. – V. 50100. – P. 1-18.
[35] Venus Flagship Mission Concept: A Decadal Survey Study/P Beauchamp, MS Gilmore, RJ Lynch et al.//2021 IEEE Aerospace Conference (50100). – 2021. – V. 48. – №. – 2326. – P. 1–18.
[36] Glaze, L. O. R. I., et al. "Venus Mobile Explorer (VME): a Mission Concept Study for the National Research Council Planetary Decacal Survey." 7th International Planetary Probe Workshop. 2010.
[37] Venus observing system. / Limaye, S., Abedin, N. M., Ao, C. O., Bocanegra, T., Bullock et al. // Bulletin of the American Astronomical Society – 2021. – V. 53. – №. 4– P. 370.
[38] Smrekar, Suzanne, et al. "Venus Origins Explorer (VOX) concept: A proposed new frontiers mission." 2018 IEEE Aerospace Conference. IEEE, 2018.
[39] Valentian, Dominique, et al. "Venus sample return mission revisited." Experimental Astronomy 54.2-3 (2022): 597-616.
[40] Agrawal R. et al. Venus cloud sample return concept for astrobiology //Advances in Space Research. – 2024. – V. 74. – №. 1. – P. 490-504.
[41] Sundararajan V. Tradespace Exploration of Space System Architecture and Design for India's Shukrayaan-1, Venus Orbiter Mission//ASCEND 2021. – 2021. – P. 4103.
[42] VERITAS (Venus Emissivity, Radio Science, InSAR, Topo-graphy And Spectroscopy): A Proposed Discovery Mission/S. Smrekar, M. Dyar, S. Hensley et al.//AAS/Division for Planetary Sciences Meeting. – 2016. – V. 48. – P. – 207–216.
[43] Garvin J.B. и др. Revealing the Mysteries of Venus: The DAVINCI Mission/J.B. Garvin, S.A. Getty, G.N. Arney et al.//The Planetary Science Journal. – 2022. – V. 3. – №. 5. – P. 117.
[44] DAVINCI+: Deep atmosphere of Venus investigation of noble gases, chemistry, and imaging plus/J. Garvin, S. Getty, G. Arney et al.//Journal of Atmospheric Sciences. – 2020. – V. 3. – №. – 2326. – P. – 2599.
[45] Garvin, James B., et al. "Revealing the mysteries of Venus: The DAVINCI mission." The Planetary Science Journal 3.5 (2022): 117.
[46] EnVision: Europe's proposed mission to Venus/T. Widemann, R. Ghail, C. Wilson et al.//Agu fall meeting abstracts. – 2020. – V. – 2020. – P. – P022--02.
[47] Eismont, N A, R R Nazirov, K S Fedyaev, V A Zubko, A A Belyaev, L V Zasova, D A Gorinov, and A V Simonov. 2021. "Resonant Orbits in the Problem of Expanding Accessible Landing Areas on the Venus Surface." Astronomy Letters 47 (5): 316–30.
[48] Eismont, Natan, Vladislav Zubko, Andrey Belyaev, Konstantin Fedyaev, Lyudmila Zasova, Dmitry Gorinov, Alexander Simonov, and Ravil Nazirov. 2022. "Expansion of Landing Areas on the Venus Surface Using Resonant Orbits in the Venera-D Project." Acta Astronautica 197 (March): 310–22. https://doi.org/10.1016/j.actaastro.2022.03.014.
[49] Zubko, Vladislav A., et al. "A method for constructing an interplanetary trajectory of a spacecraft to Venus using resonant orbits to ensure landing in the desired region." Advances in Space Research 72.2 (2023): 161-179.
[50] Wilmer, Adam P., et al. "Sun–Venus CR3BP, part 1: periodic orbit generation, stability, and mission investigation." *Archive of Applied Mechanics* 94.4 (2024): 921-941.
[51] Bettinger, Robert A., Adam P. Wilmer, and Jacob A. Dahlke. "Sun–Venus CR3BP, part 2: resonance investigation and planar periodic orbit family generation." *Archive of Applied Mechanics* 94.3 (2024): 625-650.
[52] Kosenkova, A. V. 2021. "Investigation of Reachable Landing Sites in the 'VENERA-D' Mission for Various Types of a Lander." In AIP Conference Proceedings. Vol. 2318. https://doi.org/10.1063/5.0035839.
[53] Kosenkova, Anastasia, and Victor Minenko. 2020. "Investigation of Various Lander's Configurations Possibilities Capable of Manoeuvring Descent to the Venus Surface." In Proceedings of the International Astronautical Congress, IAC. Vol. 2020-October.
[54] Vorontsov, V. A., M. G. Lokhmatova, M. B. Martynov, K. M. Pichkhadze, A. V. Simonov, V. V. Khartov, L. V. Zasova, L. M. Zelenyi, and O. I. Korablev. 2011. "Prospective Spacecraft for Venus Research: Venera-D Design." Solar System Research 45 (7). https://doi.org/10.1134/S0038094611070288.
[55] Breakwell, John V, and Lawrence M Perko. 1966. "Matched Asymptotic Expansions, Patched Conics, and the Computation of Interplanetary Trajectories." In Progress in Astronautics and Rocketry, 17:159–82. Elsevier. https://doi.org/10.1016/B978-1-4832-2729-0.50015-6.
[56] Casalino, Lorenzo, Guido Colasurdo, and Dario Pastrone. 1998. "Optimization of DV Earth-Gravity-Assist Trajectories." Journal of Guidance, Control, and Dynamics 21 (6): 991–95.

[57] Prado, A. 2007. “A Comparison of the ‘Patched-Conics Approach’ and the Restricted Problem for Swing-Bys.” Advances in Space Research 40 (1): 113–17. https://doi.org/10.1016/j.asr.2007.01.012.
[58] Bate, Roger R., et al. Fundamentals of astrodynamics. Courier Dover Publications, 2020.
[59] Li, Jin, Jianhui Zhao, and Fan Li. 2018. “A New Method of Patched-Conic for Interplanetary Orbit.” Optik 156 (March): 121–27. https://doi.org/10.1016/j.ijleo.2017.10.153.
[60] Sukhanov A.A. Universal solution of Lambert’s problem.//Cosmic Research. 1989. – V. – 26. – №. 4. – P. 415–423.
[61] Izzo, Dario. 2015. “Revisiting Lambert’s Problem.” Celestial Mechanics and Dynamical Astronomy 121 (1): 1–15. https://doi.org/10.1007/s10569-014-9587-y.
[62] Papkov, O. Multiple Gravity Assist Interplanetary Trajectories (1st ed.). Routledge. 1998. – 292 p.
[63] Golubev, Yu F., A. V. Grushevskii, I. P. Kiseleva, V. V. Koryanov, A. G. Tuchin, and D. A. Tuchin. 2019. “Main Property of the Jacobi Integral for Gravity Assist Manoeuvres in the Solar System.” Solar System Research 53 (6). https://doi.org/10.1134/S0038094619060029.
[64] Golubev, Yu F., A. V. Grushevskii, V. V. Koryanov, A. G. Tuchin, and D. A. Tuchin. 2018. “Mission Design of Multipurpose Flights to Venus.” Journal of Computer and Systems Sciences International 57 (6). https://doi.org/10.1134/S1064230718060059.
[65] Golubev, Yu F., A. V. Grushevskii, V. V. Koryanov, A. G. Tuchin, and D. A. Tuchin. 2019b. “Synthesizing Spacecraft Orbits with High Inclinations Using Venusian Gravity Assists.” Doklady Physics 64 (1): 24–26. https://doi.org/10.1134/S1028335819010087.
[66] Golubev, Yu F., A. V. Grushevskii, V. V. Koryanov, A. G. Tuchin, and D. A. Tuchin. 2020. “A Universal Property of the Jacobi Integral for Gravity Assists in the Solar System.” Cosmic Research 58 (4). https://doi.org/10.1134/S0010952520040061.
[67] Strange, Nathan, Ryan Russell, and Brent Buffington. 2008. “Mapping the V-Infinity Globe.” Advances in the Astronautical Sciences 129.
[68] Takubo, Yuji, Damon Landau, and Brian Anderson. "Automated tour design in the Saturnian system." *Celestial Mechanics and Dynamical Astronomy* 136.1 (2024): 8.
[69] Simonov A.V., Kovaleva S.D., Gordienko E.S., Pol V.G., Kosenkova A.V. Features of trajectory design of prospective spacecrafts for Venus exploration.Venus research. Engineering Journal: Science and Innovations, 2021, issue 10. http://doi.org/10.18698/2308-6033-2021-10-2122 (in Russian)
[70] Vallado, David A. 2016. “Fundamentals of astrodynamics and applications.” Journal of Chemical Information and Modelling 53 (9).
[71] Hughes K.M. Gravity-assist trajectories to Venus, Mars, and the ice giants: Mission design with human and robotic applications. //PhD thesis. – Purdue University, 2016. 158 p.
[72] Lidov, M. L. (1962). The evolution of orbits of artificial satellites of planets under the action of gravitational perturbations of external bodies. Planetary and Space Science, 9(10), 719-759.
[73] Prokhorenko, V. I. "Study of satellite situations mission." Acta Astronautica 10.7 (1983): 499-503.
[74] Battin, R. H. An Introduction to the Mathematics and Methods of Astrodynamics, Revised Edition. American Institute of Aeronautics and Astronautics, Reston ,VA, 1999.
[75] Bate, R. R., Mueller, D. D., White, J. E., and Saylor, W. W. Fundamentals of Astrodynamics. Dover Publications, Garden City, New York, 2020.
[76] Lidov, M. L. "Evolution of the orbits of artificial satellites of planets as affected by gravitational perturbation from external bodies." AIAA Journal 1.8 (1963): 1985-2002.
[77] Orbit design for launching INTEGRAL on the Proton/Block-DM launcher/Eismont N.A. et al.//Astronomy and Astrophys. – 2003. – V. 411. – №. 1. – P. L37--L41.
[78] Zubko, Vladislav, and Andrey Belyaev. "A simplified analytical approach for determining eclipses of satellites occulted by a celestial body." Acta Astronautica 220 (2024): 374-391.